



HAL
open science

Dielectric and Optical Characterizations of Insulating Coatings Prepared by Micro-Arc Oxidation Process on Aluminum Space Parts

J. Kighelman, H. Cerda, L. Arurault, Gilbert Teyssedre, Laurent Boudou, P. Combes, J. Tschember

► **To cite this version:**

J. Kighelman, H. Cerda, L. Arurault, Gilbert Teyssedre, Laurent Boudou, et al.. Dielectric and Optical Characterizations of Insulating Coatings Prepared by Micro-Arc Oxidation Process on Aluminum Space Parts. ICPADM 2009: 9th International Conference on Properties and Applications of Dielectric Materials, Harbin, China, Jul 2009, Harbin, China. pp.1110-1113, 10.1109/ICPADM.2009.5252307 . hal-03942704

HAL Id: hal-03942704

<https://hal.science/hal-03942704>

Submitted on 18 Jan 2023

HAL is a multi-disciplinary open access archive for the deposit and dissemination of scientific research documents, whether they are published or not. The documents may come from teaching and research institutions in France or abroad, or from public or private research centers.

L'archive ouverte pluridisciplinaire **HAL**, est destinée au dépôt et à la diffusion de documents scientifiques de niveau recherche, publiés ou non, émanant des établissements d'enseignement et de recherche français ou étrangers, des laboratoires publics ou privés.

Dielectric and Optical Characterizations of Insulating Coatings Prepared by Micro-Arc Oxidation Process on Aluminum Space Parts

J. Kighelman¹, H. Cerda¹, L. Arurault¹, G. Teyssedre²,
L. Boudou², P. Combes³, J. Tschember⁴

¹CIRIMAT-LCMIE, Université Paul Sabatier, 118 route de Narbonne,
31062 Toulouse Cedex 9, France

²LAPLACE, Université Paul Sabatier, 118 route de Narbonne,
31062 Toulouse Cedex 9, France

³GIT, 1 et 7, rue Joseph-Marie Jacquard, 31270 Cugnaux, France

⁴ASTRIUM, 31 rue des Cosmonautes 31400 Toulouse, France

Abstract: *The optical and electrical properties of aluminum oxide layers for potential application in spacecrafts have been investigated. We have correlated the operational conditions of the Micro-Arc Oxidation (MAO) process to the structural features of the coatings and to the optical properties. Our results show that for appropriate electrolyte formulation the thermo-optical parameters of the coatings could fit the specification range for cold coatings used in space applications. Furthermore, the electrical properties of such coatings have been investigated by means of surface and volume conductivity measurements as well as dielectric spectroscopy. Results show that materials exhibiting the best thermo-optical properties are those having the higher electrical conductivity, with values appearing favorable regarding the targeted application.*

Keywords: Aluminum oxide, MAO process, dielectric and optical properties.

INTRODUCTION

In orbit, satellites are exposed to significant thermal variations. To ensure reliable operation of their on-board systems and equipment, a thermal control of the space-craft is necessary using cold, neutral or warm coatings. For very specific missions, like solar orbiter, cold coatings, also called "white coatings", are used. They exhibit specific optical properties (solar absorbance < 0.2 and IR emissivity > 0.8). Furthermore, to prevent any electrostatic discharge problems, due to implanted charge accumulation under space radiations, coatings also need to have specific electrical properties, such as low resistivity.

The aluminum oxides obtained from MAO process, which are typically used in the fields of wear resistance as well as thermal and electrical insulation, could exhibit thermo-optical properties compatible with space environment specification.

MATERIALS AND CHARACTERISATION TECHNIQUES

Samples were prepared using MAO process on aluminum substrate. MAO is an electromechanical surface treatment consisting of thick crystalline oxide growing on a metallic substrate [1-2]. Different coatings obtained with different process conditions, were optically and electrically tested. The main process parameters are summarized in Table 1.

Table 1: Process parameters for coatings preparation. (f=frequency, J=current density, t= process duration, Cs=silicate concentration) d = substrate thickness. J and Cs are given in relative value for confidentiality purpose.

Sample	J (r.u.)	t (min)	Cs (r.u.)	d (μm)
#1	J_1	150	C_1	200
#2	$2.4xJ_1$	50	$6xC_1$	2000
#3	$1.5xJ_1$	30	$6xC_1$	1000
#4	$2.8xJ_1$	30	$6xC_1$	1000

Structural characterization of the coatings was achieved by a set of techniques ranging from XRay diffraction, thermogravimetric analysis –TGA-, differential thermal analysis –DTA- and Electron Probe MicroAnalyser (EPMA).

To compare the optical properties of different coatings the solar absorbance α and the thermal emissivity ε were measured using an absorptiometer and an emissiometer (EL510 and EL520 Elan Informatique). α quantifies the amount of solar rays absorbed by the coating and ε the coating capacity to convert its thermal energy into ray.

For DC current measurements, an aluminum top electrode, 12mm in diameter, was deposited on the sample surface by CVD (chemical vapor deposition) while the ground electrode was the aluminum substrate. Current measurements were carried out under vacuum (10^{-1} Pa) at room temperature by means of a Keithley 617 ammeter. The surface resistivity was measured using the concentric ring probe configuration. The inner electrode and the guarded ring were deposited by CVD. Impedance measurements were performed using a

Dielectric Spectrometer (Novocontrol Alpha-a) in the temperature range -100°C to 200°C and in the frequency range 10^{-1} to 10^6 Hz. Like for DC measurements, Al electrodes were used. To compare the different samples a simple RC model is used to extract important parameters like the resistivity at low frequency and the dielectric constant for a fixed frequency and at a given temperature.

RESULTS AND DISCUSSION

Optical measurements

Table 2 gives the optical parameters of the coatings. As can be seen in the table, samples #2 and #4 have optical properties complying with the specification of a cold coating. The comparison between table 1 and 2 indicates that high current density and high silicate concentration are required to obtain good optical properties. This observation is confirmed by complementary results on the impact of process parameters on the final optical properties of the coatings, not presented here for space saving.

Table 2: Thickness, solar absorbance α and thermal emissivity ϵ of the coatings.

Sample	Coating Thickness (μm)	α (± 0.04)	ϵ (± 0.04)	Cold coating specification
#1	95	0.47	0.77	$\alpha < 0,2$ $\epsilon > 0,8$
#2	100	0.10	0.83	
#3	50	0.27	0.76	
#4	100	0.17	0.77	

Electrical measurements

DC characterization

Figure 1 shows typical current transients obtained when applying voltage steps in the range 0 to 100 V followed by short-circuit steps. The polarization time was fixed to 10 minutes and can be considered as leading to a representative conduction current. The volume resistivity values, estimated from the value of the current at the end of the polarization step, and obtained from a linearization of the I(V) data are given in Table 3, along with surface resistivity results.

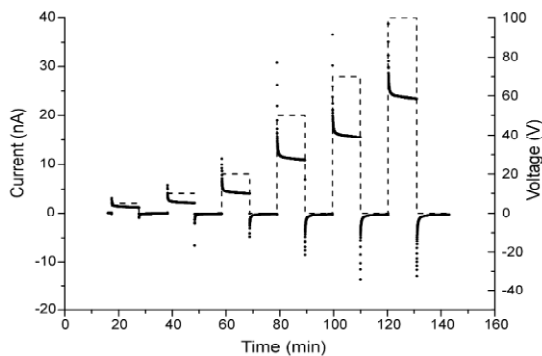


Figure 1: Transient currents for sample #4 at room temperature.

Table 3 shows that the surface and volume resistivities of sample #1 are more than two orders of magnitude higher

when compared to the three others. Thereafter the dynamic dielectric characterization results are presented for samples exhibiting the highest and lowest volume resistivity values, i.e. samples #1 and #4.

Table 3: DC electrical characteristics of coatings.

Sample	Volume resistivity ($\Omega\cdot\text{m}$)	Surface resistivity (Ω/\square)
#1	$4.1\cdot 10^{12}$	$1\cdot 10^{16}$
#2	$6.4\cdot 10^9$	$5\cdot 10^{11}$
#3	$8.6\cdot 10^9$	$2\cdot 10^{12}$
#4	$2\cdot 10^9$	$3\cdot 10^{11}$

Dynamic characterization

Figures 2 and 3 show the modulus of the impedance, $|Z|$, along with the phase angle between applied voltage and current, as a function of frequency, for samples #1 and #4. For an ideal capacitor, the impedance varies linearly as $1/f$ and the phase angle is -90°C . For sample #4, the variation of $|Z|$ shows a resistor behavior for low frequency and high temperature. In the high frequency domain and for all the temperatures investigated a capacitive behavior is revealed. This behavior allows us to estimate a volume resistivity that can be compared to DC measurement previously presented, and the dielectric permittivity in the region of capacitive behavior. The dielectric permittivity varies from 14 to 15 for temperatures in the range -100°C to 200°C .

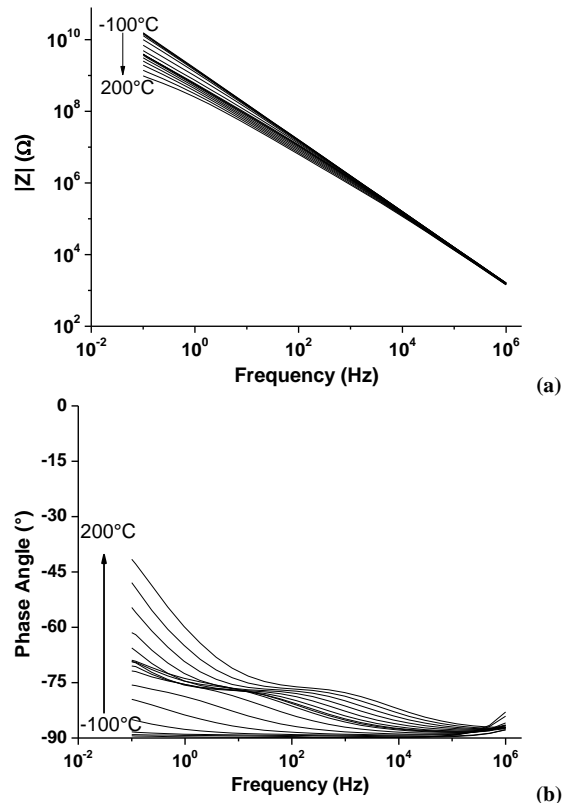


Figure 2: Variation of the impedance modulus (a) and phase angle between voltage and current, (b), as a function of frequency for different temperatures for sample #1. Data are given in temperature steps of 20°C .

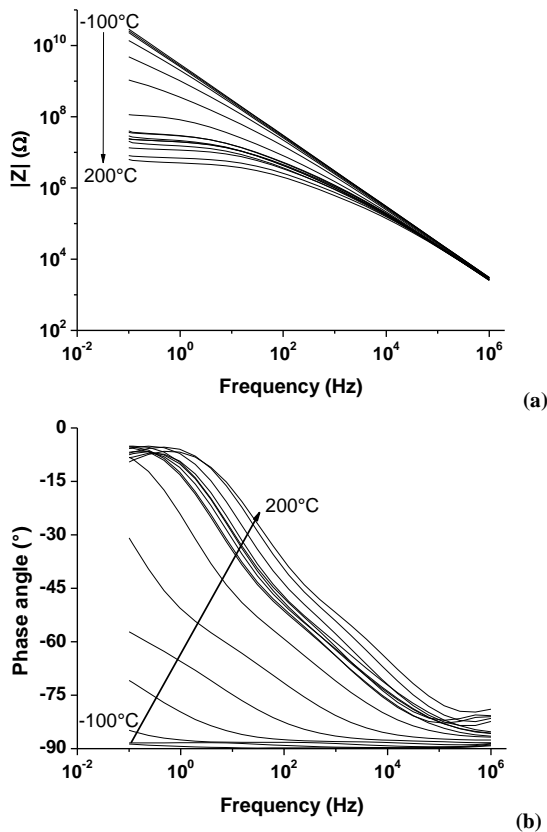


Figure 3: Variation of the impedance modulus (a), and phase angle between voltage and current (b), as a function of frequency for different temperatures for sample #4. Data are given in temperature steps of 20°C.

The volume resistivity calculated at 20°C and 0.1 Hz (Table 4) is about $6.5 \cdot 10^7 \Omega \cdot m$ and is significantly lower than the value calculated from DC measurements at room temperature (Table 3). We assume that this difference can be due to the presence of water within the coating during the measurement. Indeed, DC measurements were carried out under vacuum whereas a nitrogen flux is injected for dynamic measurements without prior outgassing. In order to study this point a thermal treatment was applied prior to dynamic dielectric measurements. The results are presented in the next section.

For sample #1, the frequency range explored is not large enough to see a resistive behavior in the low frequency domain, but the resistivity can be estimated to a value higher than $3 \cdot 10^9 \Omega \cdot m$. From the high frequency domain the dielectric constant was calculated. It varies from 26 to 30 for temperatures varying from -100°C to 200°C. Sample #1 shows a higher volume resistivity, as expected from DC data and a higher dielectric constant compared to sample #4. In both cases, the values are higher than that of bulk alumina (typically $\epsilon_r = 8-9$). The porosity of coatings, defective regions in the structure (cf. discussion) and possibly water inclusion, along with some uncertainty regarding coating thickness might explain such difference.

Table 4: Dielectric parameters extracted from the variation of $|Z|$ vs. frequency and temperature.

Sample	Volume resistivity (at 20°C)	Relative permittivity (-100 to 200°C)
#1	$> 3 \cdot 10^9 \Omega \cdot m$	26-30
#2	$6.5 \cdot 10^7 \Omega \cdot m$	14-15

Thermal treatment effect on optical and dielectric properties

Sample #4 is the most appropriate sample for a space application as cold coating, because of its good optical properties and low conductivity compared to the other tested samples. In the following, we investigate the effect of a thermal treatment on both optical and electrical properties.

For dielectric measurements, the thermal treatment consists of an in situ annealing at 200°C for 1 hour. Figure 4 shows the corresponding results. The peak observed at around 100°C on $|Z|$ for the untreated sample can be due to the presence –and possibly release– of water within the coating. After the thermal treatment, this peak disappears, and the value of the impedance increases, clearly indicating an increase in the resistivity of the material.

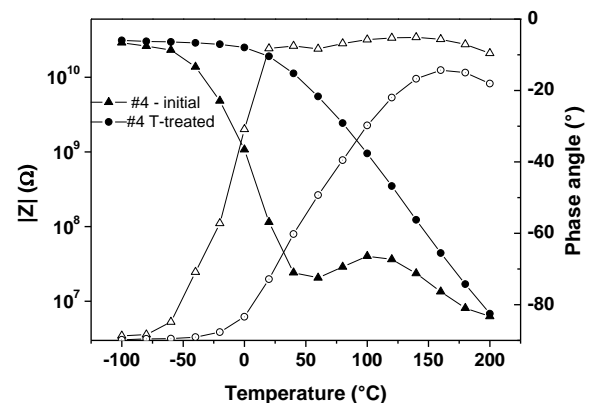


Figure 4: Impedance (solid symbols) and phase angle (open symbols) measured at 0.1Hz as a function of temperature prior to (triangles) and after (circles) thermal treatment on sample #4.

For optical properties, the thermal treatment consisted in annealing samples under air atmosphere at 200°C or 400°C for 5 hours. The thermo-optical properties were measured at room temperature under vacuum to avoid water absorption along with after storage in air at room temperature. The results shown in Table 5 do not reveal any significant variation of the optical properties after heating or after storage in air, pointing towards stable optical properties of the coatings.

Table 5: Impact of thermal treatment and of subsequent storage in air on thermo-optical properties of sample #4.

Sample #4	$\alpha (\pm 0.04)$		$\epsilon (\pm 0.04)$	
	vacuum	7days / air	vacuum	7days / air
untreated	0.17		0.77	
5h at 200°C	0.10	0.12	0.85	0.89
5h at 400°C	0.17	0.14	0.73	0.88

DISCUSSION

Changes in dielectric properties of the coatings with process conditions may have several origins, resorting to the porosity, to the water uptake and to composition of the coatings. Various structural characterizations have been implemented to sort out the possibilities. First, X-ray diffraction patterns indicate that the layers are constituted of several crystalline phases. To sum-up, an increase in silicate content of the electrolyte favors the formation of silicate phases in the coatings: the ratio of alumina (Al_2O_3) to silicate (Al_2SiO_5 -called mullite-) is around 90:10 in sample #1 and 50:50 in the others. An important point is that large silicate content induces an increase in the amorphous phase fraction of the coatings (cf. broad band in the region 15-30° in Fig.5).

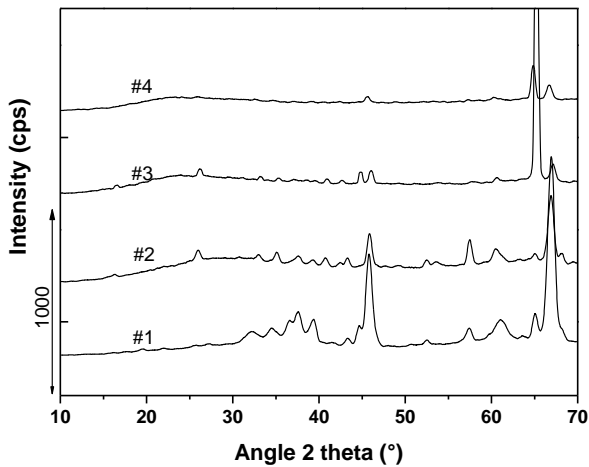
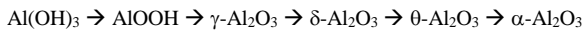


Figure 5: X-Ray diffraction patterns of the samples

Voigt and co-authors [3] studied the correlation between chemical composition and electrical properties of rf sputtered alumina films. They found that the leakage current increases with the concentration of OH groups, which act as defect sites. As OH groups are presumably located preferentially in the amorphous phase, the way of investigating it consisted in combining TGA and DTA. Table 6 shows the weight losses in the sample interpreted as arising from free water release, and from the known thermodynamic stability of aluminas given, in increasing order of stability, as:



The lower losses of water associate with OH groups in sample #1 appear to reflect the higher crystalline phase content for this material. It can be seen that electrical resistivity decreases as the concentration of Al(OH)_3 and AlOOH groups increases, being the higher for sample #4. Therefore, the presence of OH groups could explain the lower electrical resistivity of coatings.

Finally, the good thermal stability of the coatings deserves to be mentioned: the weight losses for temperature increase up to 1400°C is in the range 0.6 to 2.3%, about 20% of it corresponding to loss of adsorbed water.

Table 6: Weight losses (in weight %) attributed to water of the various samples as obtained by TGA. Temperature intervals were defined according to the range of thermal stability of the corresponding groups.

Sample	Adsorbed water (<=100°C)	Al(OH)_3 (100-400°C)	AlOOH (400-700°C)
#1	0.12	0.22	0.13
#2	0.35	0.83	0.54
#3	0.22	0.50	0.25
#4	0.57	1.12	0.60

CONCLUSION

We have correlated the operational conditions of the Micro-Arc Oxidation (MAO) process to the dielectric and thermo-optical properties of coatings grown onto Al substrates. The main outputs of the study are as follows:

i/ Strong variation in electrical conductivity of the coatings were obtained depending on process conditions. Relatively low electrical resistivity materials can be processed, which appears promising for space application.

ii/ Low resistivity appears to go with appropriate thermo-optical properties; the low resistivity could be associated to the presence of OH groups in the coatings.

iii/ However, resistivity appears to increase significantly with thermal treatment of the coatings. This feature has to be investigated in more detail, considering water release and possible hydroxyl groups removal with thermal treatments.

REFERENCES

- [1] A.L. Yerokhin, X. Nie, A. Leyland, A. Matthews and S.J. Dowey, "Plasma electrolysis for surface engineering", *Surface and Coatings Technology*, vol. 122, pp. 73-93, 1999.
- [2] A.L. Yerokhin, A. Shatrov, V. Samsonov, P. Shashkov, A. Pilkington, A. Leyland and A. Matthews, "Oxide ceramic coatings on aluminium alloys produced by a pulsed bipolar plasma electrolytic oxidation process", *Surface and Coatings Technology*, vol. 199, pp. 150-157, 2005.
- [3] M. Voigt, A. Bergmaier, G. Dollinger and M. Sokolowski, "Correlation of chemical composition and electrical properties of rf sputtered alumina films", *J. Vacuum Sci. Technol. A*, vol. 27, pp. 234-244, 2009.

ACKNOWLEDGEMENTS

We are imbedded to Region Midi-Pyrenees for support to this work. GIT and ASTRIUM acknowledge the European Spatial Agency for their support.